Clays and Clay Minerals, Vol. 39, No. 1, 70–76, 1991.

GENESIS AND MORPHOLOGY OF IRON SULFIDES IN GRAY KAOLINS

G. NORMAN WHITE,[1] J. B. DIXON,[1] R. M. WEAVER,[2] AND A. C. KUNKLE[2]

[1] Department of Soil and Crop Sciences, Texas A&M University
College Station, Texas 77843

[2] J. M. Huber Corporation, Huber, Georgia 31298

Abstract—Many of the presently oxidized Georgia kaolins probably existed originally in the reduced (gray) state. For that reason, the distribution of iron sulfides in presently gray kaolins may elucidate features observed in oxidized kaolins. An understanding of the nature of gray kaolins may also aid in the development of processing strategies for the exploitation of these abundant resources. The size, morphology, and degree of crystallite bonding of iron sulfides (pyrite and marcasite) in three gray kaolin cores from the Macon, Georgia kaolin district were examined by X-ray powder diffraction, X-ray fluorescence, scanning electron microscopy, and other physical and chemical methods. Pyrite and marcasite were identified as dominantly gravel- and sand-size equant crystals and crystal aggregates, rather than as framboids. Pyrite crystals commonly showed rough octahedral faces, which extended over minor cube faces. Locally, spiral growth dislocations were also observed. Marcasite was found in radiating, prismatic, and tabular crystals. In general, the marcasite crystal aggregates were much more fragile than those of pyrite. The dominance of octahedral crystal shapes and textures of the pyrite suggest inorganic precipitation from solutions supersaturated with respect to octahedral crystal faces.

Key Words—Kaolinite, Marcasite, Morphology, Oxidation, Pyrite, Scanning electron microscopy, Sulfide.

INTRODUCTION

Kaolins containing significant amounts of sulfides and organic matter are termed "gray kaolins." Gray kaolin deposits may prove to be valuable kaolin reserves should methods of beneficiation be developed. The size, morphology, and compactness of sulfides in gray kaolins are therefore important variables in the design of beneficiation techniques. The physical properties of the sulfides in gray kaolins may also provide information on the origin of the kaolins.

Previous research (Hurst, 1979; Schrader *et al.*, 1983) has suggested that many of the oxidized kaolins presently mined in the Coastal Plain of the Southeastern United States were at one time reduced (i.e., gray), but have since been oxidized. The field trip guide for the 1979 annual meeting of The Clay Minerals Society (Hurst, 1979) shows scanning electron micrographs (SEMs) of pyrite from a kaolin deposit in the Twiggs clay at the Hobbs Mine, which was being mined by the Thiele Kaolin Company at the time of that meeting. The pyrite morphology shown in the SEMs was that of submicrometer-size framboids made up of discrete pyrite octahedra. Also, cubes and pyritohedrons were reported, but these forms were less common. Other portions of the field trip guide (Hurst, 1979) also noted the existence of nodular pyrite in kaolins. No systematic studies describing the particle size ranges, distribution within a deposit, mineral composition, or morphology of sulfides found in gray kaolins, however, have been published.

Pyrite in sediments has been the subject of many studies (see, e.g., Berner, 1984; Berner and Raiswell, 1984), focusing on the importance of organic material and sulfate on its formation. Bacterially decomposable organic material has been shown to be important not only as an energy source for the bacterial reduction of sulfate to H_2S, but also as an agent for producing anoxic conditions in the sediment (Berner, 1984). The ratio of organic carbon to sulfur (C/S ratio) has been used as a method of distinguishing the depositional environment of a sediment (Berner, 1984; Berner and Raiswell, 1984). Berner (1984) also concluded that the sulfate concentration is not a limiting factor in the rate of sedimentary pyrite formation if the concentration is >5 mM. The sulfate concentrations of most marine anoxic sediments exceed this concentration, but the values for most fresh water sediments do not. Berner (1984) found that availability of reactive organic matter was the limiting factor in the formation of sedimentary pyrite in marine sediments and that the availability of sulfate limited pyrite formation in freshwater sediments. He further concluded that the available source of iron may be limited in some environments to the iron in hydrous oxides, because oxides are more soluble than other iron-containing phases.

The morphology of iron sulfides was not studied by Berner or his colleagues. Murowchick and Barnes (1989), however, systematically studied the effects of temperature and supersaturation on pyrite morphology under hydrothermal conditions. They found that screw-dislocation and layer-by-layer growth were the most common growth mechanisms in pyrite, with continuous growth mechanisms being of only minor importance. At low supersaturations, screw dislocation-controlled growth was dominant; nucleation and lateral

Copyright © 1991, The Clay Minerals Society

https://doi.org/10.1346/CCMN.1991.0390109 Published online by Cambridge University Press

spreading on the growing surface (layer-by-layer growth) became dominant as the degree of supersaturation increased. They concluded that the rate of crystal growth was limited by either the rate at which components are incorporated (surface control) or the rate at which ionic components diffuse to the surface of the pyrite (diffusion control). Surface controlled growth, thought to be dominant in aqueous solutions, results in equant, euhedral crystals. During diffusion controlled growth, any protrusion of a crystal surface may extend into a region of increased concentration. As a result, growth at the ends of the crystal is favored, and a dendritic crystal morphology results. Murowchick and Barnes (1989) also concluded that the degree of supersaturation expressed itself in pyrite morphology; e.g., at low supersaturation acicular crystals were produced. The morphology changes from acicular to smooth cubes to rough cubes to octahedra to pyritohedra and finally to trapezoids as the degree of supersaturation increases. Their study, however, was performed under hydrothermal conditions with induced temperature gradients, and so the applicability of the results to sediments may not be straightforward.

The purpose of the present study was to examine the occurrence and morphology of sulfides in three gray kaolin cores from the inner Coastal Plain of Georgia in order to provide mineralogical information useful for the utilization of gray kaolins and to illuminate the genesis of these materials.

MATERIALS AND METHODS

With the cooperation of the Huber Kaolin Corporation, three cores were obtained from sites in Twiggs and Wilkinson Counties, Georgia. One core was taken in Tertiary-age deposits; the other two cores were from Cretaceous-age deposits. Selected samples were analyzed for Fe, Ti, K, and S by X-ray fluorescence (XRF) using a Cr X-ray source and a Philips PW1410 X-ray spectrometer, with the time required for a set number of counts measured. Values for pH of a 1:2.5 solid: water mixture (J. M. Huber Corporation, 1955) were obtained with a Radiometer PHM62 pH meter.

Total carbon was determined by the dry combustion technique of Allison (1965). All sample determinations were duplicated; samples high in carbon were reanalyzed to confirm the results. The method of Bundy and Bremner (1972) was used to check for the presence of inorganic carbon in the samples.

Sulfides were identified from sand fractions (0.05–2 mm) and larger concretions by X-ray powder diffraction using CuKα radiation and a Philips goniometer automated by a Databox system and Materials Data Incorporated software.

Sulfide morphology was studied with JEOL JSM-25SII And JSM-T330A scanning electron microscopes (SEMs) and a JEOL JSM-35CF scanning electron microscope equipped with an energy-dispersive X-ray fluorescence spectrometer (SEM/EDX). These samples were prepared by sprinkling the mineral particles on a SEM sample stub that had been covered with double-sided tape. Samples used for morphology determinations were coated with gold-palladium; those used for chemical determinations were coated with carbon.

Two kaolin samples, one containing pyrite and one containing marcasite, were dispersed in pH 10 water and fractionated; the sulfur contents of the particle-size fractions were determined by XRF in the same manner as for the bulk samples.

RESULTS

The Tertiary kaolin deposit was located under 12 m of overburden. The upper 3 m of the deposit consisted of cream-colored kaolin containing scattered 3–5-mm-size ocher colored blotches and 5–10-cm-size yellow mottles. The cream kaolin-gray kaolin interface was abrupt and not coincident with the slope of the land surface. Immediately below this interface, the deposit contained finely dispersed pyrite, and, within 20 cm of the interface, 3–5-mm-size pyrite particles were visible. The gray kaolin was brittle and had a pisolitic character with small linear blotches about 1 mm across and 4 mm long in a near-vertical orientation. The deposit became grayer with depth, and locally sulfide nodules were present several centimeters in size. Gray mottles were similar in size and shape to the yellow mottles in the cream-colored kaolin above. Beneath about 8 m, the kaolin became gritty with quartz sand, and sampling was terminated.

Cretaceous kaolin site I had 24 m of overburden. At this site, the kaolin was gray and contained nodules of marcasite at the overburden-kaolin interface. The gray kaolin had abundant 1–20-mm-size sulfides throughout. An abrupt interface with red kaolin was found at about 4.5 m beneath the top of the deposit. The red kaolin was highly mottled with 5–50-mm-diameter yellow and white mottles. Sampling was terminated about 2 m into the red kaolin. Cretaceous kaolin site II had 18.5 m of overburden. The upper 25 cm of the kaolin deposit contained thin (1–3 mm), dark gray and ocher-colored layers underlain by a uniform, 8.75-m-thick, gray layer underlain in turn by red kaolin. Much of the gray part of this deposit was very brittle; sulfide nodules were very common, some of which were several centimeters in size. Some zones contained abundant sand-size sulfide grains. Sampling was discontinued after 1 m into the red kaolin.

The pH of dried subsamples from the Tertiary site ranged between 3.8 and 5.2 (Figure 1a). The pH of subsamples from Cretaceous site I increased with depth from 4.5 at the surface of the kaolin to almost 6.5 at 4.3 m beneath the surface (Figure 1b). The pH of the subsamples from Cretaceous site II ranged between 3 and 6.5 (Figure 1c). Some of the variability in pH may have been the result of oxidation after coring.

https://doi.org/10.1346/CCMN.1991.0390109 Published online by Cambridge University Press

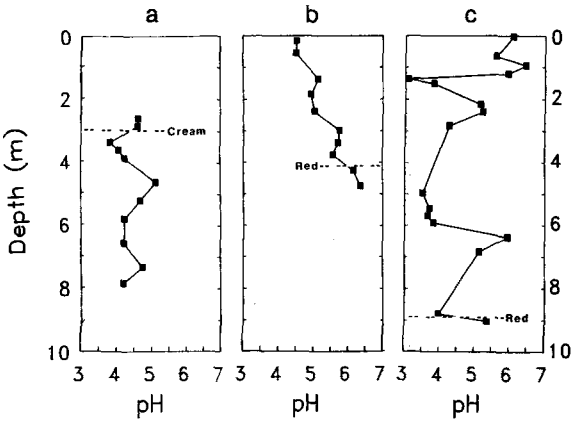

Figure 1. Initial pHs of samples as a function of depth from the top of the deposit. a. Tertiary kaolin site. b. Cretaceous site I. c. Cretaceous site II.

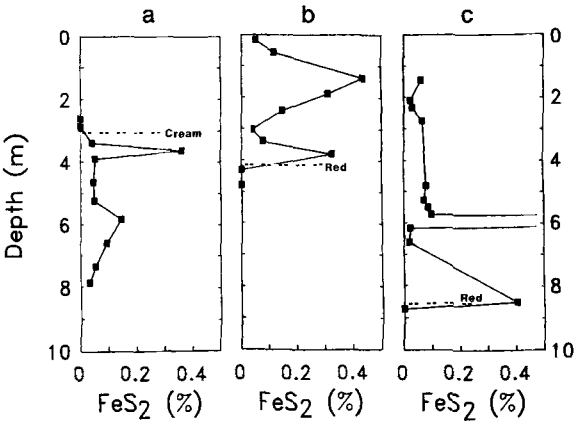

Figure 2. Concentrations of FeS_2 (based on total S) for samples as function of depth from top of deposit. a. Tertiary kaolin site. b. Cretaceous kaolin site I. c. Cretaceous kaolin site II.

The carbon contents were much higher than would have been expected from samples having Munsell color values of ≥7 (Table 1). The organic carbon was uniform at about 0.1% for the Tertiary site, but ranged between 0.09 and 0.59% for the Cretaceous sites. Inorganic carbon analyses to detect siderite (Bundy and Bremner, 1972) were negative.

The sulfide content, based on total sulfur content, is low (generally <1% FeS_2 by weight) (Figure 2). XRD of nodular sulfides and sand fractions revealed that many of the samples contained both pyrite and marcasite, with one sulfide being present only in a trace amount relative to the concentration of the other.

Two samples, one from Cretaceous site II, containing a high concentration of pyrite and little or no marcasite, and the other from Cretaceous site I, containing marcasite and no pyrite were examined. These samples were size fractionated to determine the concentrations of sulfides as a function of particle size. The FeS_2 tended to be concentrated in the coarser size fractions (Table 2). Many marcasite grains were fragile having a loose texture, and were commonly broken during separation. By comparison, pyrite was more compact and survived fractionation without apparent damage. These observations, along with observations of particle morphology using SEM, suggest that the marcasite in the finer-size fractions was in large part due to disaggregation of the fragile particles during size fractionation.

Pyrite was found in all samples near the center of the gray kaolin layer. The predominant crystal form for pyrite was the octahedral form (Figures 3a–3d, 3f, and 3h), with less prominant cube faces in some (Figures 3a–3c, and 3h). Radiating crystals having obvious octahedral faces were common (Figures 3d and 3e). Some octahedral crystals showed obvious growth dislocations (Figure 3f). The cubic form of pyrite was suggested by an indentation in a kaolin vermiform in one sample, but was not otherwise observed (Figure 3i). Compact masses of pyrite were common (Figure

Table 1. Organic carbon in gray kaolins as determined by dry carbon train.[1]

Sample depth[2] (m)	Organic carbon (%)
Tertiary site	
2.6	0.10 (cream)
4.5	0.12
6.6	0.13
7.4	0.12
Cretaceous site I	
1.4	0.59
2.4	0.29
3.3	0.28
4.0	0.33
5.1	0.10 (red)
Cretaceous site II	
0.3	0.09
0.9[3]	0.09
2.1	0.09
5.6	0.14
8.8	0.46 (red)

[1] Allison (1965) dry carbon train method used.
[2] Depths measured from the top of the kaolin deposit.
[3] Subsample of locally concentrated yellow bands within the core at this depth.

Table 2. Particle size distribution and sulfide size distribution for pyrite- and marcasite-containing kaolin samples.

	Pyrite-containing sample[1]		Marcasite-containing sample[2]	
Size fraction	Particle size (%)	Sulfide size distribution (%)	Particle size (%)	Sulfide size distribution (%)
>2 mm	3.3	86.9	<0.1	44.7
2 mm–50 μm	5.1	11.9	7.6	13.8
50–2 μm	27.9	0.8	40.4	20.4
2–0.2 μm	59.1	0.4	51.1	19.9
<0.2 μm	4.6	<0.1	0.9	1.2

[1] Sample from 6.2 m depth at Cretaceous site II.
[2] Sample from 3.4 m depth at Cretaceous site I.

https://doi.org/10.1346/CCMN.1991.0390109 Published online by Cambridge University Press

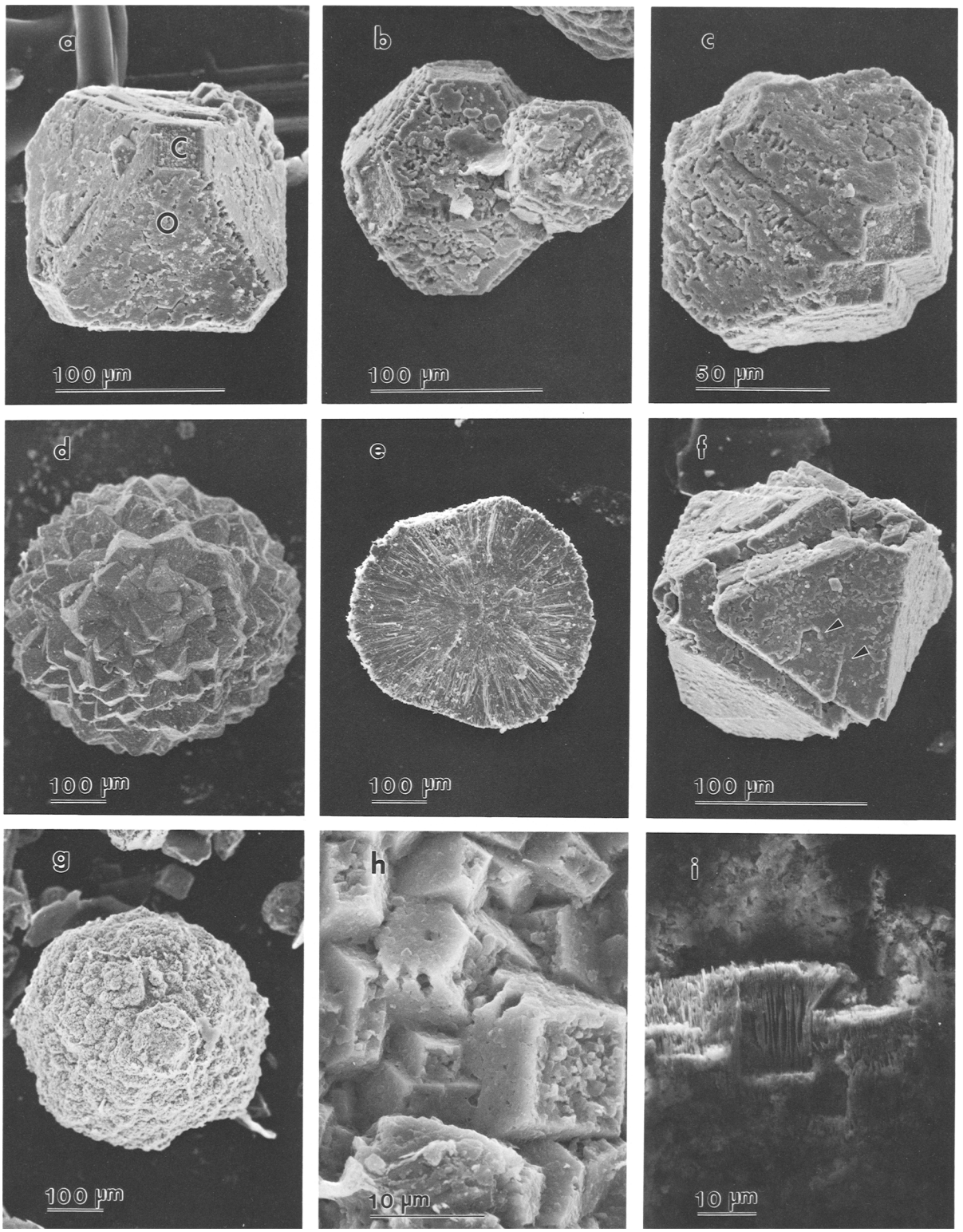

Figure 3. Scanning electron micrographs of pyrite shapes in gray kaolins: a. pyrite particle showing octahedral (O) and cube (C) faces; b. pyrite grain with octahedral faces protruding over cube face; c. intergrown pyrite grain with prominent octahedral faces protruding over cube faces; d. spheroidal pyrite with many octahedral faces; e. interior of pyrite particle showing radiating growth pattern; f. spiral growth patterns (arrows) on intergrown pyrite particle; g. pyrite aggregates showing no visible crystal faces at whole grain resolution; h. higher magnification of grain (g) showing octahedral faces protruding over degraded cube faces; i. cubic indentation in kaolinite vermiforms suggesting prior pyrite morphology.

https://doi.org/10.1346/CCMN.1991.0390109 Published online by Cambridge University Press

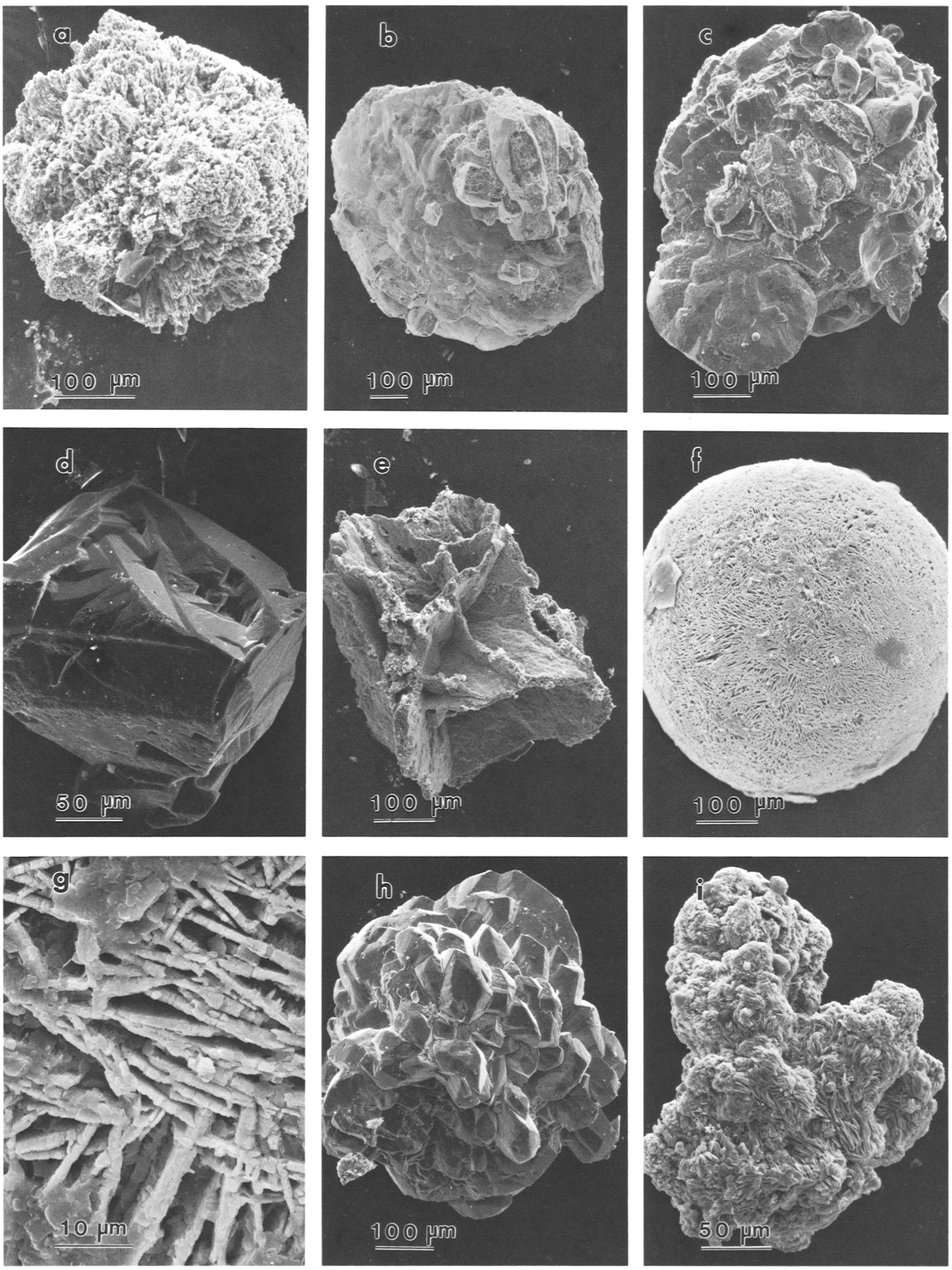

Figure 4. Scanning electron micrographs of marcasite shapes and porosity: a. radiating growth pattern of marcasite crystals; b. globular marcasite particle; c. marcasite showing characteristic cockscomb morphology; d. marcasite showing etch pits and characteristic rounded faces; e. marcasite aggregate made of coarsely intergrown tabular crystal masses; f. spheroidal marcasite aggregate of intergrown platy particles; g. enlargement of (f); h. marcasite grain showing well-formed, terminated prism faces; i. marcasite particle with many cockscomb surfaces.

https://doi.org/10.1346/CCMN.1991.0390109 Published online by Cambridge University Press

3g). Higher magnification SEMs showed that the aggregates invariably were covered with intergrown octahedra (Figure 3h). Many of these aggregates were globular and showed growth rings in the interior if broken (Figure 3e). No discrete framboidal pyrite was observed.

Marcasite was common, generally as the dominant sulfide mineral, in several samples near the oxidizing boundaries at the top and bottom of the Cretaceous cores. Marcasite morphologies were quite different from those observed for pyrite. Globular and radiating crystals were usually less compact than for pyrite (Figures 4a and 4b). Characteristic rounded "cockscomb" crystal forms (Figure 4c) and crystals having curved faces were common (Figures 4c, 4d, and 4h). Tabular crystals were common, either coarsely or finely intergrown (Figures 4e–4g). Many of the particles appeared to be quite fragile and were easily damaged during size fractionation. Some particles showed prismatic growths (Figure 4h). As noted for the pyrite, some marcasite crystal faces appeared smoother than others, probably because of differences in solubility of the different crystal faces (Figures 4c, 4d, and 4h).

DISCUSSION

The oxidized surface of the kaolin deposit at the Tertiary site was in agreement with Kesler's (1963) observation that kaolins having overburdens between 8 and 15 m thick may have been oxidized in the upper portion. The higher sulfide content immediately below the oxidized zone suggests that sulfate leached from above into the reduced zone and precipitated as iron sulfide (Figure 2a).

Very little work has been done on marcasite crystal forms to help explain its occurrence in this environment. Whether the existence of marcasite is related to redox conditions, as suggested by its occurrence near the oxidizing - reducing interface, or to temporary lower pHs accompanying short-term oxidation is unknown.

Octahedral faces were the most prominent crystal faces observed on both the macrocrystalline and the microcrystalline pyrite. The octahedron faces on the microcrystalline aggregates tended to be smooth, whereas the cube faces were heavily pitted. The octahedral faces commonly extended out from the edges of the crystals overhanging the cube faces (Figure 3h). The octahedral crystal morphology had many surface steps and protruding corners and edges that suggest a relatively high level of solution supersaturation with respect to pyrite or at least to those surfaces (Murowchick and Barnes, 1989). A plausible hypothesis for the dominance of octahedral over cube faces may be a disequilibrium between the concentrations of Fe^{2+} and H_2S in solution. The octahedral face of pyrite can be formed entirely of either Fe or S_2 ions, whereas cube faces have equal amounts of Fe and S_2.

Inasmuch as the surface free energy of a crystal face is related to the concentration of the ions on the surface relative to the concentration of the ions in the solution, the octahedral face should dominate in solutions with Fe/S ratios far from unity. The cube face, on the other hand, should dominate if the ions were in equal concentrations in solution. This apparent disequilibrium could be the result of an environment in which the sulfide ion was being oxidized to sulfate or in which an excess of Fe^{2+} existed relative to H_2S. The high concentration of Fe in the red kaolin directly beneath the gray kaolin suggests that Fe was not limiting.

The most obvious source of Fe for the sulfides in the original sediment was probably iron oxides and oxyhydroxides deposited with the kaolinite in the deposit. The principal source for Fe in the gray kaolins during the recrystallization of the sulfides was probably mica. Mica in the gray kaolins is inversely related to the concentration of sulfides (White and Dixon, unpublished data), suggesting Fe sulfide formation at the expense of mica. No readily identifiable source of sulfur exists, except for the water percolation from outside the deposit. The low organic carbon content suggests that microbial action may have previously oxidized most of the original carbon present or that little carbon was originally present. Whether the deposits were closed systems with respect to O_2, Fe^{2+}, and S_2^{2-} is not known. The reduced conditions in the deposits, which are surrounded by oxidized sandy deposits, suggest little influx of O_2. The inorganic reduction of Fe^{3+} to Fe^{2+} is, however, very slow at low pHs (Singer and Stumm, 1970). Whether Fe in pyrite was leached from outside of the deposit, released by recrystallization of minerals within the deposit, or from detrital oxides is not clear. The presence of crystal faces that protrude into solution suggest localized regions of supersaturation. Because the pyrite octahedral faces tend to protrude over the cube faces, the source of the sulfides for the recrystallization of the pyrite into macroscopic octahedra may have been the cube faces of pyrite, often of the same particles. The mica content in the sample is diminished in regions in which the sulfides were recrystallized, suggesting that some of the iron came from that source.

The coarse particle size of the sulfides suggests that the kaolinite may be beneficiated by removal of the sulfides by particle size segregation, if the method does not reduce the size of fragile marcasite grains.

REFERENCES

Allison, L. E. (1965) Total carbon: in *Methods of Soil Analysis, Part 2, Agronomy 9,* C. A. Black, D. D. Evans, J. L. White, L. E. Ensminger, and F. E. Clark, eds., Amer. Soc. Agron., Madison, Wisconsin, 1367–1378.

Berner, R. A. (1984) Sedimentary pyrite formation: An update: *Geochim. Cosmochim. Acta* **48,** 605–615.

Berner, R. A. and Raiswell, R. (1984) C/S method for distinguishing freshwater from marine sedimentary rocks: *Geology* **12,** 365–368.

https://doi.org/10.1346/CCMN.1991.0390109 Published online by Cambridge University Press

Bundy, L. G. and Bremner, J. M. (1972) A simple titrimetric method for the determination of inorganic carbon in soils: *Soil Sci. Soc. Amer. Proc.* **36,** 273–275.

J. M. Huber Corporation (1955) *Kaolin Clays and their Industrial Uses:* J. M. Huber Corporation, New York, 214 pp.

Hurst, V. J., ed. (1979) *Field Conference on Kaolin, Bauxite, and Fuller's Earth:* Fieldtrip Guide, Annual Meeting of The Clay Minerals Society, 1979, 107 pp.

Kesler, T. L. (1963) Environment and origin of the Cretaceous kaolin deposits of Georgia and South Carolina: *Ga. Geol. Surv. Bull.* **6-A,** 204 pp.

Murowchick, J. B. and Barnes, H. L. (1989) Effects of temperature and degree of supersaturation on pyrite morphology: *Amer. Mineral.* **72,** 1241–1250.

Schrader, E. L., Long, A. L., Muir, C. H., Quintus-Bosz, R., and Stewart, H. C. (1983) *General Geology and Operations of Kaolin Mining in the "Southeastern Clay Belt": A Perspective from Huber, Georgia:* Field Trip Guide, 112th Annual Meeting, A.I.M.E., Atlanta, Georgia, 23 pp.

Singer, P. C. and Stumm, W. (1970) Oxygenation of ferrous iron: *U.S. Depart. of Int. Water Quality Admin., Water Pollution Cont. Res. Series Rept.* **14010-06/69,** 197 pp.

(Received 12 May, 1990; accepted 3 October, 1990; Ms. 2007)

https://doi.org/10.1346/CCMN.1991.0390109 Published online by Cambridge University Press